Progress In Electromagnetics Research C, Vol. 73, 105–113, 2017

Microstrip Magnetic Dipole Yagi Antenna with Enhanced Impedance Bandwidth and Reduced Size for Wideband Wireless Applications

Tian Li[1, *], Fu-Shun Zhang[1], Fei Gao[2], Qi Zhang[3], and Yan-Li Guo[4]

Abstract—A microstrip magnetic dipole Yagi antenna with the feasibility of obtaining a wider bandwidth and relatively smaller size is proposed and demonstrated. The proposed antenna, consisting of a reflector, a driver with backed soldered SMA connector, a coupling microstrip line with three rectangular slots and three modified directors, is designed and fabricated. Good agreement between simulated and measured results is observed. Simulated and measured results reveal that the proposed antenna can provide an impedance bandwidth of 19.2% (4.95–6 GHz). Meanwhile, within the impedance bandwidth, the radiation pattern of the proposed antenna has front-to-back (F/B) ratios ranging from 10.1 dB to 26.1 dB, cross-polarization levels in the endfire direction from 47.1 dB to 73.0 dB, peak gains from 6.4 dBi to 10.4 dBi with an average peak gain of 9.6 dBi and endfire gains from 2.2 dBi to 4.3 dBi with an average endfire gain of 3.1 dBi. Additionally, the measured bandwidth of 19.2% (4.95–6 GHz) not only meets the need for certain Wi-Fi (5.2/5.8 GHz) or WiMAX (5.5 GHz) band communication application, but also provides the potential to implement multiservice transmission.

1. INTRODUCTION

Microstrip magnetic dipole Yagi antennas have attracted great attention due to their merits of simplicity in structure, low profile, light weight, low fabrication cost, broad bandwidth, realizing unidirectional radiation with high gain and vertical polarization, and suitability for integration with microwave circuits [1–8]. With the inherent vertical polarization characteristic, when microstrip magnetic dipole Yagi antennas are employed in the communication systems on a horizontal platform, such as ground-wave communications, transmitter and receiver can keep the same vertical polarization for good connection when the transmitter or receiver rotates on the platform. Otherwise, connection would be affected or even disrupted, when the transmitter and receiver employ horizontal polarization. Meanwhile, due to their double-sided printed structures, they are suitable for some applications with a metal plane below them. With more director elements, they can be applied in point-to-point communications that need a narrow beam at endfire with vertical polarization as well. Moreover, since the feature of broad bandwidth is becoming increasingly necessary due to the high data rate required by modern services, some newly published microstrip magnetic dipole Yagi antennas in [6–8] focus on the realization of broad bandwidth with various microstrip magnetic dipole Yagi antenna structures. In [6], a low-profile 4-element Yagi array based on microstrip magnetic dipole antennas with vertical polarization achieves an impedance bandwidth of 13.1% around 5.21 GHz, whereas its size of $2.08\lambda_0 \times 1.91\lambda_0$ is not compact. In [7], a compact magnetic Yagi antenna with vertical polarized radiation was presented using the substrate integrated waveguide (SIW) technology. The SIW functions as the driven element to generate vertically

Received 19 February 2017, Accepted 9 April 2017, Scheduled 14 April 2017

* Corresponding author: Tian Li (tianli@stu.xidian.edu.cn).

[1] National Key Laboratory of Antennas and Microwave Technology, Xidian University, Xi'an 710071, China. [2] Electrical and Computer Engineering Department, University of California at San Diego, La Jolla, USA. [3] Institute of Information Science and Technology, Beijing University of Chemical Technology, Beijing 100029, China. [4] Institute of Science, Air Force Engineering University, Xi'an 710077, China.

polarized wave and realize miniaturization, and the design of reflector is omitted. The proposed antenna in [7] obtains an impedance bandwidth of 16.15% and a compact size of $1.58\lambda_0 \times 0.95\lambda_0$. In [8], a compact vertically polarized microstrip Yagi antenna based on the half-mode substrate integrated waveguide (HMSIW) technology obtains an impedance bandwidth of 10.5% and a very compact size of $1.82\lambda_0 \times 0.57\lambda_0$.

In this paper, a relatively compact microstrip magnetic dipole Yagi antenna with a measured impedance bandwidth of 19.2% and size of $1.46\lambda_0 \times 1.27\lambda_0$ is presented. Each element of the five-element microstrip magnetic dipole Yagi array is on the basis of a rectangular microstrip patch with one long edge opened and the other three edges shorted, thereby working as a magnetic dipole. A coupling microstrip line is introduced between the driven element and the first-stage director element to enhance their mutual coupling, which effectively improve the front-to-back (F/B) ratio performance, especially for the middle and upper frequencies. Meanwhile, by symmetrically loading three pairs of shorting vias on the three-stage director, both impedance and pattern bandwidths are greatly enhanced at upper frequency band. Finally, three rectangular slots are symmetrically loaded on the coupling microstrip lineso as to further enhance the impedance bandwidth. For demonstration, the proposed antenna is fabricated and measured. The measured results have a reasonable agreement with the simulated ones.

2. ANTENNA CONFIGURATION

As shown in Figure 1, the proposed antenna can be divided into four parts, namely reflector, driver, coupling microstrip line and three directors. The substrate is 80.2 mm×69.6 mm×1.5 mm in size, and its relative dielectric constant and loss tangent are 2.2 and 0.0009, respectively. Each magnetic dipole array element is realized by a microstrip patch with one long edge opened and the other three edges shorted. For fabrication convenience, several rows of closely-spaced shorting pins penetrating through the proposed antenna are employed to replace the ideal shorting walls. The shorting pins have a same radius of 0.3 mm, while they have two different distances of 1 mm and 1.5 mm. The driver is 63 mm ×9.8 mm in size. Meanwhile, the feeding point locates in the center of the driver in lateral direction and has a distance of 3.6 mm from the driver's opened edge. The reflector is 69.6 mm×10.1 mm in size and has a same lateral dimension with that of the substrate. The distance between the driver and reflector is 14.05 mm. The director consists of three stepped stages. Their sizes are 62.8 mm×8 mm, 52.5 mm×7.9 mm and 42.2 mm×7.85 mm, respectively. Moreover, they have a same spacing of 12.05 mm. The coupling microstrip line introduced between the driver and the first-stage director is 69 mm×14.4 mm in size. Furthermore, three pairs of shorting vias symmetrically loaded on the three-stage director have a same distance of 17 mm from the short shorted edges of three stepped directors. Additionally, three rectangular slots symmetrically etched on the coupling microstrip line have the same size of 14.4 mm×0.5 mm. Finally, an annular slot with an outer radius of 1.5 mm is etched on bottom ground plane acting as an isolation structure for welding convenience. The detailed geometry and dimensions of the proposed antenna are given in Figure 1 and Table 1.

3. ANTENNA DESIGN

The mechanism of the magnetic dipole can be interpreted as follows. First, all the array elements of the five-element microstrip magnetic dipole Yagi array are based on a rectangular microstrip patch with one long edge opened and the other three edges shorted. Second, the patch with three edges shorted works as a cavity-backed slot antenna. The cavity is generated by the upper patch, the metal ground, and the rows of shorting pins. The opened edge equals to a narrow slot. When the cavity is excited, there is an electric field produced at the slot in the vertical direction. According to the principle of equivalent magnetic current, a magnetic current is generated at the slot and the radiation is mostly from the opened edge. Therefore, the long shorted edge enables each rectangular microstrip antenna to be a magnetic element, which provides vertically polarized radiation at endfire. While the other two shorted edges are extra designs to prevent propagation or leakage at these ends. Third, the patch has a longitudinal size along $+X$-axis direction of normally $\lambda_{g0}/4$. And the patch has a lateral size along $+Y$-axis direction of about one wavelength. Meanwhile, the cavity placed in the substrate sideway makes the profile much lower, which is only $0.027\lambda_0$. Furthermore, for the parasitic elements, the longitudinal

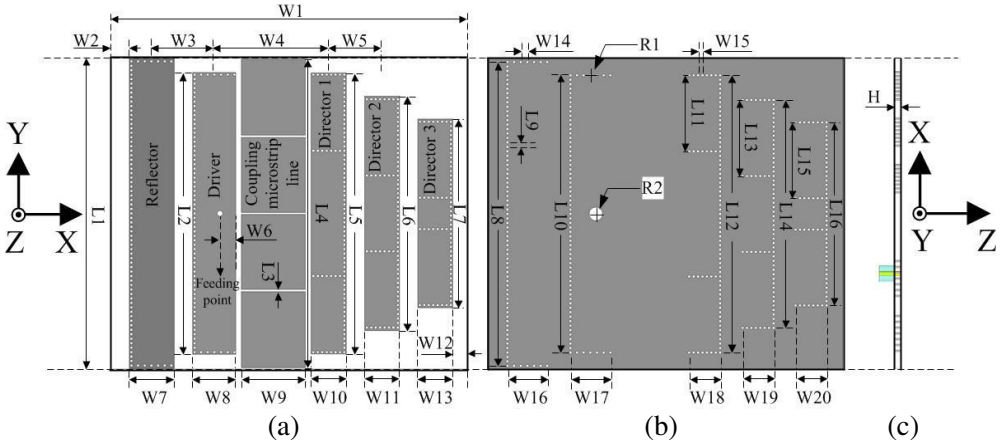

Figure 1. Configuration of the proposed antenna. (a) front view; (b) back view;(c) side view.

Table 1. Dimensions of the proposed antenna. (Unit: mm).

Parameter	Value	Parameter	Value	Parameter	Value
L1	69.6	L14	51	W11	7.9
L2	63	L15	17	W12	3.25
L3	0.5	L16	41	W13	7.85
L4	69	W1	80.2	W14	1.5
L5	62.8	W2	4.1	W15	1
L6	52.5	W3	14.05	W16	9
L7	42.2	W4	25.8	W17	9
L8	68	W5	12.05	W18	7
L9	1	W6	3.6	W19	7
L10	62	W7	10.1	W20	7
L11	17	W8	9.8	R1	0.3
L12	62	W9	14.4	R2	1.5
L13	17	W10	8	H	1.5

sizes along $+X$-axis direction of the reflector element and director elements are a little greater and less than $\lambda_{g0}/4$ respectively just as that of the classical Yagi array. Finally, with an infinite metal ground, the microstrip magnetic dipole radiates an omnidirectional radiation in the upper half of the E-plane (XZ-plane), which is contributed from the equivalent magnetic current on the opened edge.

The driver is energized directly with a backed soldered SMA connector, which makes the SMA connector have less interference with the radiated filed. While the reflector and directors act as parasitic radiators whose current are induced by mutual coupling. Moreover, the parasitic directors are used to achieve a very substantial increase with respect to gain in the forward end-fire direction compared with a simple driver. In order to have a strong coupling between the driver and the first-stage director, a rectangular coupling microstrip line is introduced between them. Its length and width have great influences on the impedance matching and F/B ratio performance, respectively. Meanwhile, as shown in Figure 2 (the surface current with red color refers to the dominant surface current), three pairs of shorting vias are symmetrically loaded on the three-stage director to break the surface current distribution surface balance, especially for that of three modified directors, hereby greatly enhancing the impedance and pattern bandwidths at upper frequency band [9]. Simultaneously, three rectangular slots

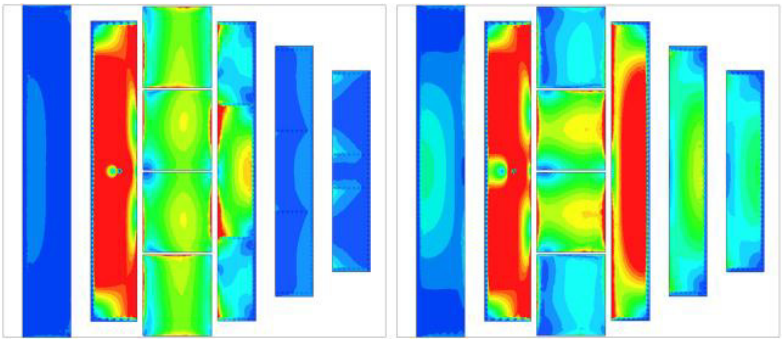

(a) (b)

Figure 2. Comparison of the surface current distributions between the proposed antenna and the one without three pairs of shorting vias. (a)/(b): with/without three pairs of shorting vias.

are symmetrically loaded on the coupling microstrip line as a perturbation structure to further improve its impedance bandwidth [10]. Furthermore, the reflector is used to reflect the transverse-electric surface wave generated by the driver. Since the resonances of the reflector and stepped director are at lower and middle/upper frequency band respectively, thus by adjusting the length of the reflector as well as the distance of the director and driver, favorable F/B ratio property at lower and middle/upper frequencies can be obtained. In addition, compared with horizontally polarized planar quasi-Yagi antennas in [11], whose main beams point exactly at endfire, the proposed antenna's main beam deviates from the endfire direction caused by the great diffraction effect of the finite ground plane.

4. SIMULATED AND MEASURED RESULTS

The measured and simulated VSWRs of the proposed antenna are depicted in Figure 3. Good agreement between the simulated and measured results is obtained. With reference to the figure, the simulated and measured impedance bandwidths (VSWR$\leq$2) of the proposed antenna are 18.8% (4.97–6 GHz) and 19.2% (4.95–6 GHz), respectively. Moreover, simulated radiation properties of the proposed antenna are shown in Table 2 and Figure 4. It is seen that relatively stable pattern characteristics are obtained within the operating band.

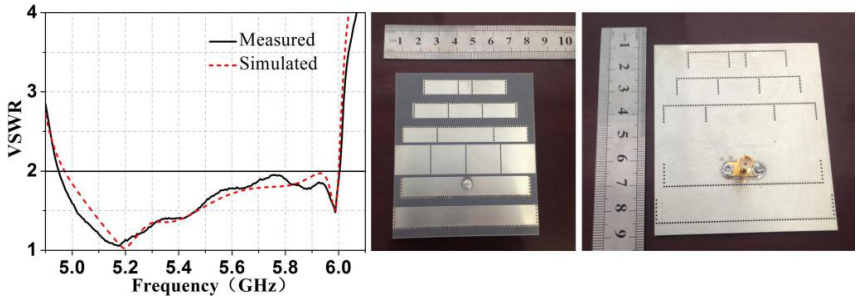

(a) (b) (c)

Figure 3. Simulated and measured VSWRs and the photographs of the fabricated antenna. (a) VSWRs; (b) front view of the fabricated antenna; (c) back view of the fabricated antenna.

Figure 4 shows the simulated and measured normalized radiation patterns in the E-plane (XZ-plane) and H-plane (XY-plane) at 5.2, 5.5 and 5.8 GHz. Compared with the simulated radiation properties shown in Table 2, the measured radiation patterns at 5.2, 5.5 and 5.8 GHz have the E-plane 3-dB beamwidths of 55.5°, 57°and 59°, H-plane 3-dB beamwidths of 58°, 49°and 41°, cross-polarization levels in the endfire direction of 60.4 dB, 55.5 dB and 73 dB, F/B ratios of 10.3 dB, 10.4 dB and 21.5 dB

Table 2. Simulated radiation properties of the proposed antenna.

Freq. (GHz)	3 dB beam width(°)		X pol. in endfire direction (dB)	F/B ratio (dB)	Deviation angle in E-plane(°)	Gain (dBi)		Radiation efficiency
	E-plane	H-plane				Peak gain	Endfire gain	
5	59.5	51	62.3	12.3	42	9.6	3.8	98.8%
5.2	65.5	52	55.8	10.2	45	9.1	3.1	99.1%
5.4	66	43	53.4	10.4	47.5	9.5	2.8	99.2%
5.6	60	41	61.1	13.1	47	10.2	3.3	99.2%
5.8	58.5	40	61.6	25.5	45	10.7	4.0	98.9%
6	65	37	46.7	10.8	38.5	6.0	2.2	91.1%

and deviation angles in the E-plane of +44.5°, +46°and +44°, respectively. In Figure 5, the measured F/B ratios, peak gains and endfire gains are from 10.1 dB to 26.1 dB with an average F/B ratio of 13.5 dB, 6.4 dBi to 10.4 dBi with an average peak gain of 9.6 dBi and 2.2 dBi to 4.3 dBi with an average endfire gain of 3.1 dBi, respectively.

5. PARAMETRIC STUDY

All critical physical parameters, such as L10, W6, L4, L3, W9, L11, L8 and W4, should be adjusted carefully to achieve a good performance. In this section, the effects of these parameters on impedance bandwidth and F/B ratio are examined to facilitate the design of a same or homogeneous antenna with different specifications. During this process, all the other parameters not mentioned stay constant as shown in Table 1.

5.1. Effects of Driver and the Position of the Feeding Point (L10 and W6)

The effects of the length of the driver and the distance of the feeding point from the driver's opened edge (L10 and W6) on the impedance bandwidth are shown in Figure 6 and Figure 7, respectively. As expected, as L10 increases, the whole operating band shifts toward lower band. Meanwhile, the effect of W6 on the impedance bandwidth is similar to that of L10. To obtain good impedance matching, L10 and W6 are set as 62 mm and 3.6 mm, respectively.

5.2. Effects of the Length of Coupling Microstrip Line and Rectangular Slots (L4 and L3)

Figure 8 and Figure 9 reveal the influence of the length of the coupling microstrip line and the widths of three rectangular slots loaded on the coupling microstrip line (L4 and L3) on the impedance bandwidth, respectively. As L4 increases to 69 mm, the impedance performance at middle and upper frequencies will be effectively improved, while the impedance performance at lower frequencies almost stays the same. Moreover, when three rectangular slots are introduced with discreetly optimized widths of 0.5 mm, the impedance bandwidth can be further broadened.

5.3. Effects of the Width of the Coupling Microstrip Line and Shorting vias (W9 and L11)

W9 means the width of the coupling microstrip line. Both the impedance bandwidth and F/B ratio are sensitive to W9. As shown in Figure 10 and Figure 11 as W9 increases, the whole impedance and pattern bandwidths shift toward lower band. While the impedance and pattern bandwidths will be deteriorated, whether the values of W9 increases or decreases. L11, L13 and L15 means the distances of three pairs of shorting vias from the short shorted edges of three stepped directors, respectively. As shown in Figure 12 and Figure 13, when they have the same values of 17 mm, the impedance and pattern bandwidths of the proposed antenna are greatly enhanced at upper frequency band, without significant degradation in

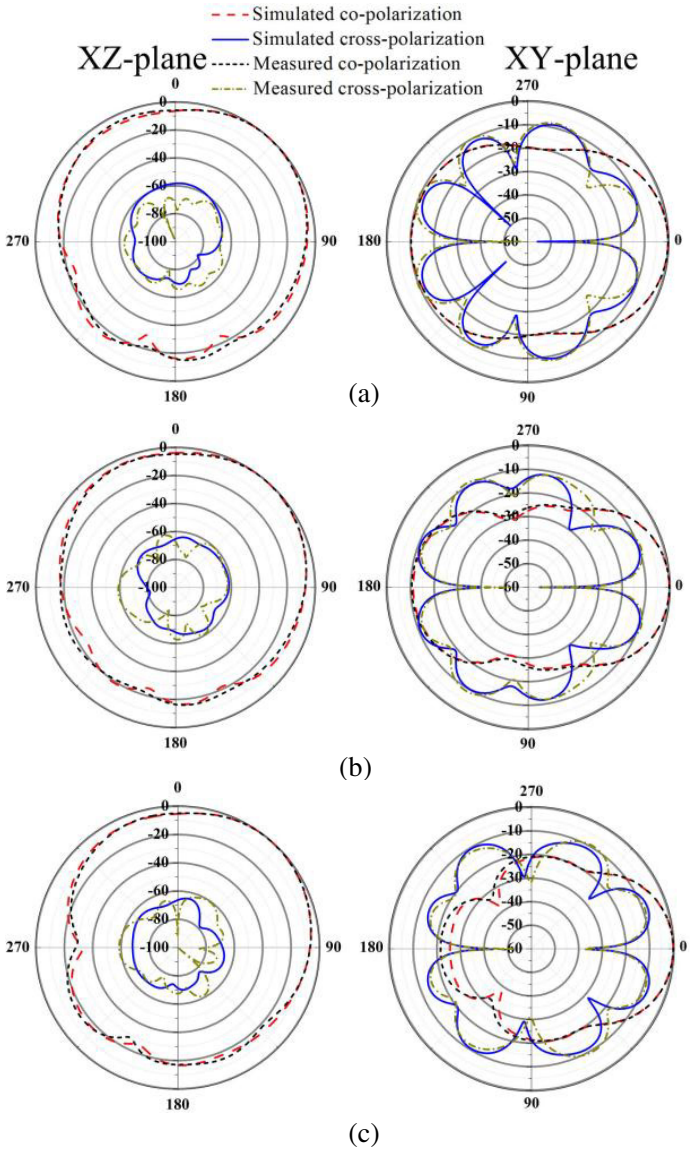

Figure 4. Simulated and measured radiation patterns in the E-plane (XZ-plane) and H-plane (XY-plane). (a) 5.2 GHz; (b) 5.5 GHz; (c) 5.8 GHz.

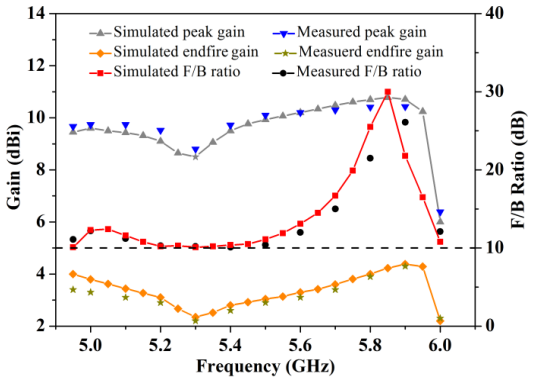

Figure 5. Simulated and measured gains and F/B ratios of the proposed antenna.

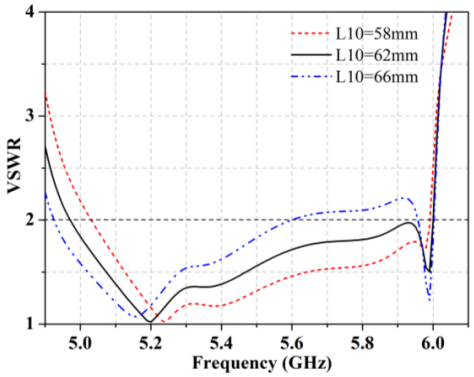

Figure 6. Simulated VSWRs with varied L10.

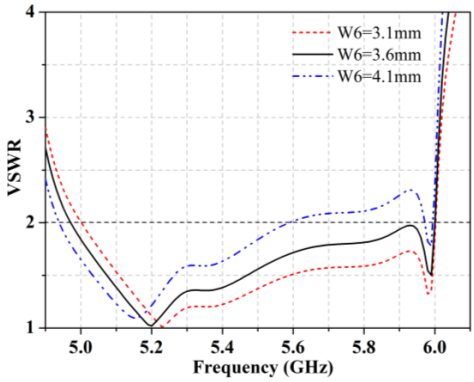

Figure 7. Simulated VSWRs with varied W6.

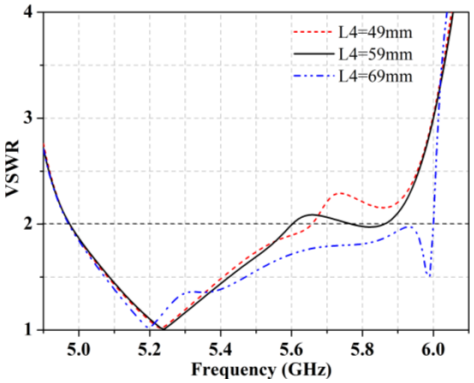

Figure 8. Simulated VSWRs with varied L4.

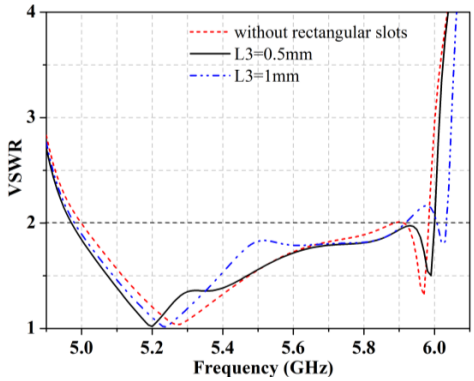

Figure 9. Simulated VSWRs with varied L3.

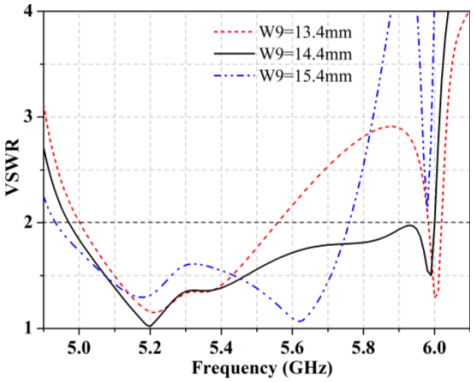

Figure 10. Simulated VSWRs with varied W9.

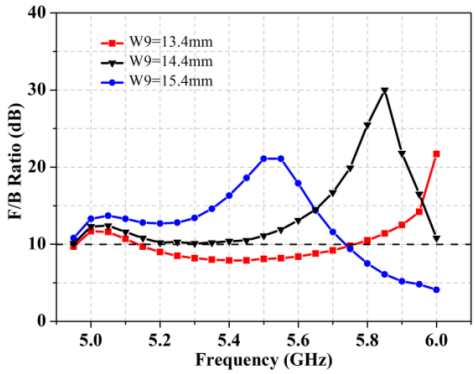

Figure 11. Simulated F/B ratios with varied W9.

impedance and F/B ratio performance for lower and middle frequency band. Consequently, the presence of these three pairs of shorting vias effectively improves the antenna performance.

5.4. Effects of Reflector and the Distance of Driver and the First-stage Director (L8 and W4)

The effects of the length of the reflector and the distance of the driver and the first-stage director (L8 and W4) on the impedance and F/B ratio performance are shown in Figure 14, Figure 15, Figure 16

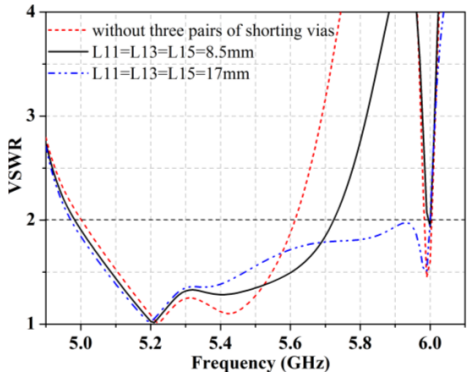

Figure 12. Simulated VSWRs with varied L11.

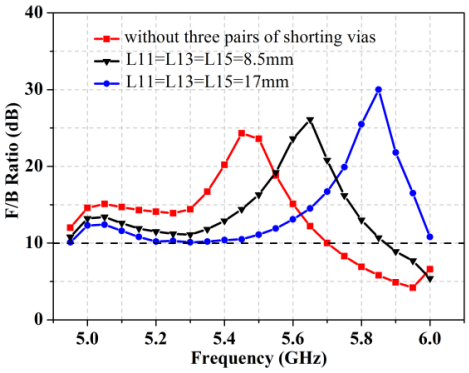

Figure 13. Simulated F/B ratios with varied L11.

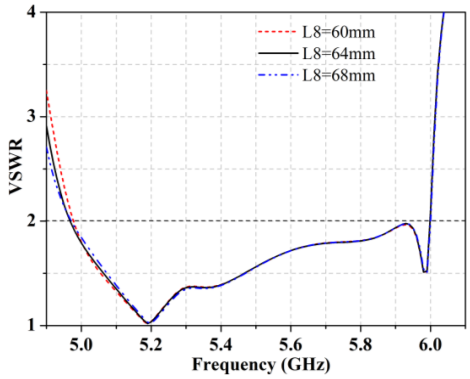

Figure 14. Simulated VSWRs with varied L8.

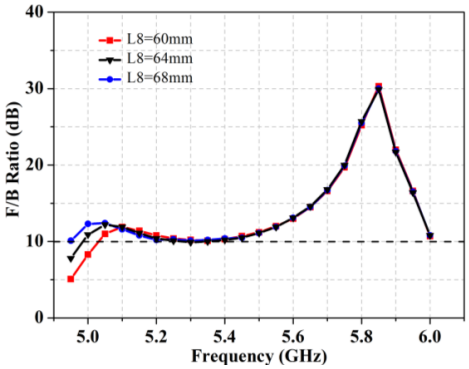

Figure 15. Simulated F/B ratios with varied L8.

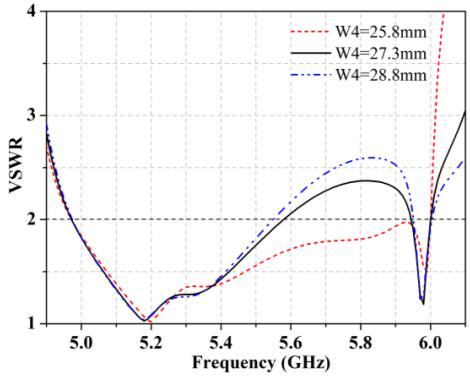

Figure 16. Simulated VSWRs with varied W4.

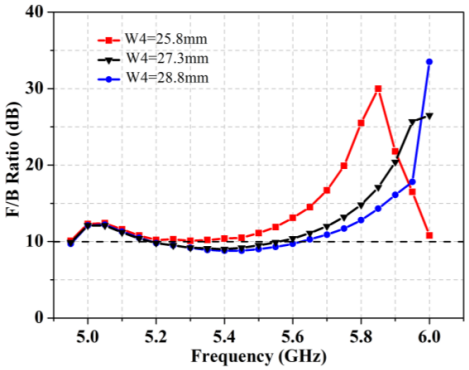

Figure 17. Simulated F/B ratios with varied W4.

and Figure 17, respectively. As shown in Figure 14 and Figure 15, as L8 increases, the F/B ratio performance at lower frequencies will be effectively improved, while the impedance matching across the whole operating band almost stays constant. Meanwhile, as shown in Figure 16 and Figure 17, as W4 increases, the performance of the impedance bandwidth and F/B ratio at middle and upper frequencies will be deteriorated. To obtain good impedance matching and F/B ratio, L8 and W4 are optimized as 68 mm and 25.8 mm, respectively.

6. CONCLUSION

A microstrip magnetic dipole Yagi antenna with enhanced impedance and reduced size has been presented. Simulation and measurement results indicate that the proposed antenna can produce an impedance bandwidth of 19.2% (4.95–6 GHz). Meanwhile, within the operating bandwidth, good F/B ratios and cross-polarization levels in the endfire direction, which are better than 10.1 dB and 47.1 dB respectively, are obtained. Relatively moderate peak gains and endfire gains, ranging from 6.4 dBi to 10.4 dBi with an average peak gain of 9.6 dBi and 2.2 dBi to 4.3 dBi with an average endfire gain of 3.1 dBi respectively, are yielded simultaneously. With these inherent characteristics, the proposed antenna can be a good candidate for wideband wireless applications.

REFERENCES

1. Ge, L. and K.-M. Luk, "A three-element linear magneto-electric dipole array with beamwidth reconfiguration," *IEEE Antennas Wireless Propag. Lett.*, Vol. 14, 28–31, Feb. 2015.
2. Ta, S.-X. and I. Park, "Crossed dipole loaded with magneto-electric dipole for wideband and wide-beam circularly polarized radiation," *IEEE Antennas Wireless Propag. Lett.*, Vol. 14, 358–361, Feb. 2015.
3. Abbosh, A., "Ultra-wideband Quasi-Yagi antenna using dual-resonant driver and integrated balun of stepped impedance coupled structure," *IEEE Trans. Antennas Propag.*, Vol. 61, No. 7, 3885–3888, Jul. 2013.
4. Yang, L., J.-D. Zhang, and W. Wu, "Wideband microstrip series-fed magnetic dipole array antenna," *Electron. Lett.*, Vol. 50, No. 24, 1793–1795, Nov. 2014.
5. Wen, Y.-Q., B.-Z. Wang, and X. Ding, "Planar microstrip endfire antenna with multiport feeding," *IEEE Antennas Wireless Propag. Lett.*, Vol. 15, 556–559, 2016.
6. Liu, J.-H. and Q. Xue, "Microstrip magnetic dipole Yagi array antenna with endfire radiation and vertical polarization," *IEEE Trans. Antennas Propag.*, Vol. 61, No. 3, 1140–1147, Mar. 2013.
7. Zhang, Z., X.-Y. Cao, J. Gao, S.-J. Li, and X. Liu "Compact microstrip magnetic Yagi antenna and array with vertical polarization based on substrate integrated waveguide," *Progress In Electromagnetics Research C*, Vol. 59, 135–141, 2015.
8. Zhang, Z., G. Zhang, X.-Y. Cao, J. Gao, H.-H. Yang, and J.-H. Wu, "Compact microstrip Yagi antenna based on half-mode substrate integrated waveguide," *2016 IEEE International Coference on Microwave and Millimeter Wave Technology*, Vol. 2, 737–739, 2016.
9. Liu, J.-H., S.-Y. Zheng, Y.-X. Li, and Y.-L. Long, "Broadband monopolar microstrip patch antenna with shorting vias and coupled ring," *IEEE Antennas Wireless Propag. Lett.*, Vol. 13, 39–42, 2014.
10. Deshmukh, A. A. and K. P. Ray,, "Formulation of resonance frequencies for dual-band slotted rectangular microstrip antennas," *IEEE Mag. on Antenna Propag.*, Vol. 54, 78–97, 2012.
11. Wu, J. N., Z.-Q. Zhao, Z.-P. Nie, and Q.-H. Liu, "Design of a wideband planar printed quasi-Yagi antenna using stepped connection structure," *IEEE Trans. Antennas Propag.*, Vol. 62, No. 6, 3431–3435, Jun. 2014.